Pergamon

European Journal of Cancer Vol. 32A, No. 3, pp. 455–460, 1996

Printed in Great Britain
0959-8049/96 $15.00+0.00

0959-8049(95)00565-X

Original Paper

Pharmacokinetics and Pharmacodynamics of Nitrosourea Fotemustine: A French Cancer Centre Multicentric Study

A. Iliadis,[1] M.-C. Launay-Iliadis,[1] C. Lucas,[2,*] R. Fety,[3] F. Lokiec,[4] B. Tranchand[5] and G. Milano[6]

[1]Faculté de Pharmacie, 27 bld Jean Moulin, 13385 Marseille Cédex 05; [2]IRIS, Division Thérapeutique Cancérologie, 6 place des Pléiades, 92415 Courbevoie Cédex; [3]Laboratoire de Pharmacocinétique, Centre René Gauducheau, bld Jacques Monod, 44805 Saint Herblain Cédex; [4]Laboratoire de Pharmacocinétique, Centre René Huguenin, 35 rue Dailly, 92211 Saint-Cloud Cédex; [5]Laboratoire de Pharmacocinétique, Centre Léon Bérard, 28 rue Laënnec, 69373 Lyon Cédex 08; and [6]Laboratoire d'Oncopharmacologie, Centre Antoine Lacassagne, 36 Voie Romaine, 06054 Nice, France

The nitrosourea, fotemustine, was given intravenously in 1 h constant-rate infusion to 66 patients in a multicentric study to assess both fotemustine pharmacokinetic behaviour and the pharmacokinetic–pharmacodynamic relationships. Depending on the tumour type treated, two administration and sampling protocols were used: 100 mg/m²/week as a conventional dose (six samples, 44 patients) and 300–500 mg/m²/day as a high dose (10 samples, 22 patients). The 91 time–concentration curves were best described by either a one-(55) or a two-compartment (36) model, and their mean clearance values did not differ significantly (85.3 ± 6.5 and 101.3 ± 9.5 l/h, respectively, $P = 0.1727$). Fotemustine pharmacokinetics were not influenced by repeated treatment (time-independence) nor by dose level (dose-independence). The pharmacodynamic effect observed on white blood cell count was expressed by a logit regression model involving the area under the curve mainly and the total administered dose. White blood cell toxicity could be predicted as a function of the dose for a given patient with a known fotemustine clearance value.

Key words: fotemustine, pharmacokinetics, pharmacodynamics, time-dependence, dose-dependence, modelling toxicity

Eur J Cancer, Vol. 32A, No. 3, pp. 455–460, 1996

INTRODUCTION

FOTEMUSTINE, a member of the chloroethylnitrosourea (CENU) class of alkylating agents, is characterised by the addition of an aminophosphonate, a bioisostere of alanine, on to the nitrosourea radical. This confers to the molecule a higher permeability through cell membranes and the blood–brain barrier [1, 2]. Its pharmacological activity, screened according to the guidelines of the National Cancer Institute, is of interest against P388 and L1210 leukaemia, colon 26 carcinoma, Lewis lung carcinoma, M5076 sarcoma and B16 melanoma [3, 4].

In the clinical setting, fotemustine has been proven active against disseminated malignant melanoma and primary brain tumours. On the basis of the phase I study [5], a specific schedule was recommended: a 100 mg/m² intravenous (i.v.) infusion over 1 h every week for 3 consecutive weeks. After a 4–5 week rest period, maintenance therapy was undertaken with 100 mg/m² every 3 weeks, in stabilised or responding patients.

In malignant melanoma patients, an objective response rate of 24.2% has been obtained with fotemustine alone [6] and 33.3% when combined with dacarbazine [7]. The median duration of response was 22 weeks (range 7–80). Reponses on visceral, non-visceral and cerebral metastatic sites, together with good tolerance to the treatment, make fotemustine a widely used drug for this indication. In patients with recurrence of a primary brain tumour, an objective response rate of 22% and stabilisation of 44.4% was observed [8].

Correspondence to A. Iliadis.
*Requests for reprints to C. Lucas.
Revised 12 Jun. 1995; accepted 5 Sep. 1995.

As for other nitrosoureas, the dose limiting toxicity of fotemustine appears as a delayed and reversible myelosuppression [9]. Although haematotoxicity is dose-related, there is a large variability in the severity of this side-effect. Interpatient variability has been observed in the pharmacokinetic (PK) parameters of fotemustine, especially concerning total body clearance [10]. Such marked variability has already been described for other anticancer agents with a more or less complex relationship between toxicity grade and concentration–time exposure [11, 12]. For instance, interesting correlations were found in clinical trials with methotrexate, 5-fluorouracil [13, 14] or carboplatin [15, 16]. Conversely, the link between pharmacokinetic (PK) variabiity and pharmacodynamics (PDs) has not been explored for the nitrosoureas. We present original data concerning fotemustine which cover different pharmacological aspects including descriptive PKs, the evaluation of time- and dose-dependence, and the PK–PD relationship.

PATIENTS AND METHODS

Patients

Between February 1990 and July 1992, 66 cancer patients (45 men, 21 women) were entered into a multicentric PK prospective study during both phase I and phase II ongoing trials with fotemustine. Written informed consent from each patient and ethics committee approval were obtained before the beginning of treatments. Eligibility criteria included performance status (Karnofsky scale) greater than 60%, objectively measurable disease, neutrophil count $> 2 \times 10^3/mm^3$, platelet count $> 10^5/mm^3$, serum creatinine < 120 mmol/l and bilirubin, ASAT, ALAT, alkaline phosphatase < 1.25 normal value.

For these patients, age, body weight and body surface area varied between 21 and 76 years, 46 and 95 kg, and 1.45 and 2 m^2, with median values of 51.5 years, 65 kg and 1.76 m^2, respectively.

Treatment protocols

Fotemustine, a diethyl-1-[3-(2-chloroethyl)-3-nitrosoureido] ethyl phosphonate, was supplied by Laboratoires Servier, France. Based on patient body surface area, the total fotemustine dose to be administered was diluted in a 5% glucose solution and intravenously infused as a 1 h constant-rate infusion. During reconstitution and administration, the infusion vial and tubing were kept protected from light.

Two different protocols were used, depending on the tumour type treated:

(1) Conventional dose fotemustine protocol (CDF protocol, phase II). Fotemustine was administered as 100 mg/m^2/week for 3 weeks to 44 patients with different tumour types: malignant melanoma ($n = 16$), colon carcinoma ($n = 14$), hepatocarcinoma ($n = 2$), renal cell carcinoma ($n = 6$) and recurrent malignant glioma ($n = 6$).

(2) High dose fotemustine protocol (HDF protocol, phase I). Fotemustine was administered at D1 and D2 at doses ranging from 300 to 500 mg/m^2/day with five steps of dose increments of 50 mg/m^2/day. At least 3 patients per dose level were sampled at D1 and D2. This protocol was used in 22 patients with recurrent malignant glioma. For all the patients receiving this protocol, an autologous bone marrow rescue was performed 72 h after fotemustine treatment to reduce the side-effects, i.e. severe neutropenia and leucopenia associated with these very high doses.

Collection of samples

From the arm not receiving the infusion, 5 ml of heparinised venous blood was collected at predetermined time points: immediately before infusion (t_0), during, and after the end of infusion. Two types of sampling protocols were used: (1) in CDF protocol: six samples at 0.25, 1, 1.25, 1.5, 1.75 and 2 h after t_0; (2) in HDF protocol: 10 samples at 0.25, 0.75, 1, 1.17, 1.25, 1.5, 1.75, 2, 2.5 and 3 h after t_0. Samples were immediately cooled on ice, centrifuged at 2000*g* at 4°C for 5 min in a refrigerated centrifuge, and plasma was quickly frozen in liquid nitrogen. Plasma was then stored at −20°C until analysis.

Analysis of samples

Intact fotemustine was assayed according to a specific procedure previously described by Gordon and associates [17], using high performance liquid chromatography on a C18 column after solid phase extraction. The UV detection was performed at 230 nm. All operations were conducted under light protection conditions. Fotemustine was measured with an overall precision of ± 5.6% and accuracy of 3.6% down to 20 ng/ml (minimum level of quantitation). Within-day variation ranged between ± 10.7% at the lowest concentration investigated (0.1 μg/ml) and ± 2.0% at 50 μg/ml. The accuracy of measurement was 108.9 and 97.6% at 0.1 and 50.0 μg/ml respectively and the response was linear up to 50 μg/ml.

An interlaboratory validation of the three different analytical centres involved in this study had previously been performed with fotemustine-spiked human plasmas, allowing all the data generated by these centres to be gathered for description of the behaviour of the compound in plasma. Coefficient of variation (CVs) for precision and accuracy were always less than 15% over the range of 50 ng/ml to 50 μg/ml; they were 15 and 19%, respectively, at the 20 ng/ml level (limit of quantitation).

Ninety-one PK profiles were obtained (66 at the first and 25 during subsequent administrations) from a total of 702 plasma samples.

Pharmacokinetics

Individual compartmental analysis. Compartmental modelling was undertaken to assess fotemustine PKs. The 91 time–concentration curves were described by either a one- or a two-compartment model using the APIS software [18]; the *F*-test [19] was used to select the adequate model. Clearance (CL in l/h), terminal half-life ($t_{1/2}$ in min) and volume of distribution at steady state (V_{dss} in l) were the estimated parameters. Area under the curve (AUC in mg/l/h) was computed as the ratio of the administered dose over the estimated individual CL.

Statistics. To compare estimated PK parameters and assess time- and dose-dependence, we performed appropriate statistical non-parametric tests (level of significance, *P*, of 0.05) with the BMDP statistical package [20]. The partitioning of one- and two-compartment kinetics within the CDF and HDF protocols was studied by a two-way frequency table on the basis of the Yates corrected χ^2 test. The PK parameters obtained with a one- or two-compartment model were compared by the Mann–Whitney test. Time-dependence was tested by the Wilcoxon matched-pair test and dose-dependence by the Kruskal–Wallis test.

Pharmacodynamics

Haematological data [haemoglobin (HEM), white blood cell count (WBC), neutrophil count (NC) and platelet count (PL)] were recorded in 34 patients (12 in the CDF and 22 in the HDF protocol) before fotemustine administration and then weekly until their respective nadir day, which usually occurred at the third week after the last course. Because of missing values in this post-treatment follow up, changes in HEM, WBC, NC and PL were recorded only on the day at which nadir occurred in 32, 32, 29 and 30 cases, respectively; they were expressed as relative values, y:

$$y = \frac{\text{(pretreatment value} - \text{nadir value)}}{\text{pretreatment value}} \quad (1)$$

Hence, y equals 0 if the haematological status is not altered by the fotemustine treatment (minimal toxicity) and equals 1 when the nadir value of the haematological parameter is zero (maximal toxicity). Because of the range of y values (between 0 and 1), the sigmoidal, or logit model was proposed as a PD model to express the variation of each haematological parameter as a function of the total given dose (Q in mg) and the total fotemustine exposure (total AUC in mg/l/h over all courses, calculated as the ratio of Q over the estimated individual CL). This model predicts y_M, the PD variable, according to the formula:

$$y_M = \frac{e^z}{1 + e^z} \quad (2)$$

where the argument z links y_M and the PK characteristics, Q and AUC. In particular, the second-order polynomial:

$$z = K_0G + C_0 + C_1Q + C_2\text{AUC} + C_3Q^2 + C_4\text{AUC}^2 + C_5Q\text{AUC} \quad (3)$$

was used to form a flexible link between y_M and, Q and AUC. In the previous expression, G is an indicator variable assigning a given patient to the CDF- or HDF-protocol group (G equal to −1 or +1, respectively). K_0, and C_0 to C_5 are the seven coefficients to be estimated by fitting the PD model (equations (2) and (3)) on the real data (equation (1)). This regression was done using the AR programme of the BMDP package. The significance of the coefficients in the regression model was investigated by means of the square root of mean squared error (RMSE in %) between observed and predicted y values. For each side-effect indicator (HEM, WBC, NC, PL), the model with minimal RMSE was retained. The number of significant coefficients was thus variable from a PD model to another. The squared multiple correlation coefficient (R^2) expressed the part of variability explained by the model. Global performances were assessed through an analysis of residuals, defined as differences between observations, y, and model predictions, y_M: lack of fit, outliers and cases with unusual influence in the model were detected on diagnostic plots.

RESULTS

Individual compartmental analysis

Among the 91 PK profiles analysed, 55 were best described by a one-compartment model and 36 by a two-compartment model. The Yates statistics rejected the hypothesis that one- and two-compartment kinetics were equally shared between CDF and HDF protocols ($P < 10^{-4}$): 34 of the 36 two-compartment kinetics resulted from patients in the HDF group. The appearance of a first very rapid decline phase (half-life α: 5.03 ± 0.9 min) within a few minutes after the end of infusion was a direct consequence of the sampling schedule used in this specific protocol (sampling times very close to one another at the end of infusion). This very short phase was hidden when CDF protocol was used because sampling times were distant from the end of infusion.

When comparing the PK parameters between the two groups (one- versus two-compartment), we noted a significant difference ($P < 0.05$) for $t_{1/2}$ and V_{dss} (Table 1). Mean CL values were similar between the two groups (85.3 and 101.3 l/h, one- versus two-compartment, $P = 0.1727$) because this short first decay phase is of little importance in the contribution to AUC. The overall mean CL was 91.7 l/h.

Time- and dose-dependence

Among the 25 available profiles, we selected only the 19 for which the same model was applicable for two consecutive courses, because $t_{1/2}$ and V_{dss} depend on the number of compartments of the model. Wilcoxon's test did not reject the hypothesis of time-independence. Hence, for further PK investigations, only 61 D1 profiles were kept in order to avoid duplication of values for patients who had a second course of treatment.

The effect of the dose on CL values was assessed in the 28 patients with recurrent malignant glioma, who were the only patients having received the CDF (6 patients) and the HDF protocols (22 patients). For the six different dose levels analysed (100, 300, 350, 400, 450 and 500 mg/m²), no significant difference in the CL was observed, indicating its dose-independence.

Pharmacokinetic–pharmacodynamic relationship

For the CDF and HDF protocols, Table 2 shows the median and the interquartile values of HEM, WBC, NC and PL distributions. The interquartile value gives a non-parametric measure of the dispersion in the data. Medians were shifted towards lower values after treatment as compared with before-treatment values. Moreover, the haematological toxicities induced by the HDF-protocol were more severe than those due to the CDF-protocol, as could be expected. For instance, in the case of WBC, the median of distribution decreased from 7.6 × 10^3/mm³ before treatment to 2.4 × 10^3/mm³ after the treatment, and from 8.05 × 10^3/mm³ to 0.6 × 10^3/mm³, respectively for CDF- and HDF-protocols. The interquartile range was also reduced by the fotemustine treatment, indicating that haematological toxicities were severe for all the patients.

Performances of PD modelling were assessed by regression R^2, RMSE (Table 3) and residual plots. Figure 1 shows the dispersion of residuals versus the predicted toxicity for HEM, WBC, NC and PL. For both the CDF and HDF protocols, residuals of predicted PL toxicity were not randomly scattered around the zero level, indicating the presence of potentially influential observations. Similarly, the model of NC did not work in the HDF protocol because it always predicts the maximum toxicity (y_M = 1). The models (NC and PL) were therefore no longer considered. Conversely, plots for HEM and WBC showed residuals randomly scattered around the zero level (RMSE equal to 8.18% and 9.59%, respectively). Only the WBC model was further investigated for two reasons:

Table 1. Mean and standard deviation of the fotemustine PK parameters: comparison between one- and two-compartment models (Mann–Whitney test)

		One-compartment $n = 55$	Two-compartment $n = 36$	P-value
CL (l/h)		85.3 ± 6.5	101.3 ± 9.5	0.1727
$t_{1/2}$(min)	α	—	5.03 ± 0.9	—
	β	17.8 ± 0.8	29.5 ± 2.3	$<10^{-4}$
V_{dss}(l)		33.7 ± 2.1	27.0 ± 2.4	0.0172

$t_{1/2}\alpha$, rapid decline phase; $t_{1/2}\beta$, slow elimination phase.

Table 2. Median and interquartile range values on haematological parameters (HEM, WBC, NC and PL) for the CDF and HDF protocols. Q_1 and Q_3 are the first and third quartiles, respectively, of the data distribution

		CDF-protocol		HDF-protocol	
		Before	After	Before	After
HEM	Median	13.50	10.80	12.80	7.80
(g %)	$(Q_3 - Q_1)$	3.32	1.40	2.50	1.14
WBC	Median	7.60	2.40	8.05	0.60
(10^3 mm^{-3})	$(Q_3 - Q_1)$	4.78	2.00	4.50	0.64
NC	Median	5.20	1.40	5.65	0.17
(10^3 mm^{-3})	$(Q_3 - Q_1)$	4.80	1.26	4.42	0.20
PL	Median	239.50	73.50	278.50	16.50
(10^3 mm^{-3})	$(Q_3 - Q_1)$	198.00	147.24	142.24	19.50

Table 3. Minimal PD regression models (minimal RMSE). R^2 expresses the part of the explained variability. For each toxicity, n is the number of cases and P the number of model parameters. Regression parameters are ordered in a descending way according to their significance in the model

	n	P	Regression coefficients	R^2	RMSE (%)
HEM	32	3	C_0, C_1, C_3	0.595	8.18
WBC	32	4	C_0, K_0, C_2, C_5	0.662	9.59
NC	29	5	C_0, K_0, C_2, C_5, C_4	0.686	9.65
PL	30	6	$C_0, C_1, C_3, K_0, C_4, C_5$	0.634	11.2

The general model is: $z = K_0G + C_0 + C_1Q + C_2\text{AUC} + C_3Q^2 + C_4\text{AUC}^2 + C_5Q\text{AUC}$ where G is a treatment indicator variable (CDF, −1; HDF, +1) and Q, the dose.

first, it is more interesting clinically because of the wide range of y predicted toxicities (0.6 up to 1 for WBC against 0.1 up to 0.4 for HEM), and second, it better fits the observed data (66.2% of the total variability explained by the WBC model against 59.5% explained by the HEM model).

The significant regression coefficients of the WBC model were the intercept C_0, and the coefficients K_0, C_2 and C_5 associated, respectively, with the distinction of CDF- and HDF-protocol groups, the total exposure AUC and its product by the dose, Q. Overall, WBC toxicity was mainly due to AUC. It is also interesting to note that, for all the models, the toxicity due to the fotemustine treatment depends on the initial haematological status, as described by equation (1).

When CL is known, one can derive AUC for a given dose Q and use the PD relationship to predict the toxicity over the range of the admissible Q values. In Figure 2, predicted WBC toxicity was simulated as a function of Q for patients from the HDF-protocol group, with median and extreme CL values. From these simulations, it appears that a high CL induces moderate toxicities, as for patient 9 (CL = 115.4 l/h, toxicity increased from 86 to 92% for a total dose ranging from 900 up to 1800 mg). Monitoring WBC toxicity is more interesting for lower CL values, since toxicity may increase from 90 up to 100%, as for patients 23 and 34 (CL = 56.4 and 82.9 l/h, respectively).

DISCUSSION

Among anticancer drugs, nitrosoureas have been the least explored for their clinical PKs [11, 21, 22]. This is probably due to their relative instability in plasma, where they are

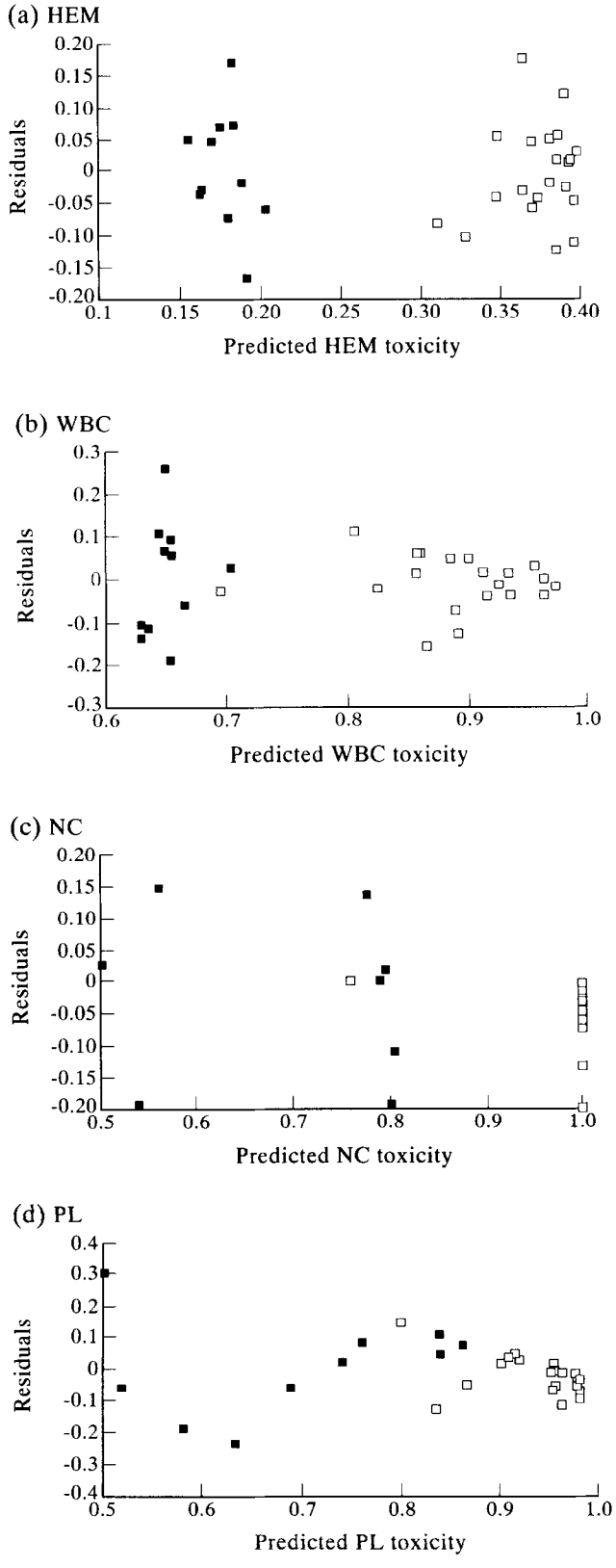

Figure 1. Residual plots for the regression PD models. ■, CDF-protocol; □, HDF-protocol.

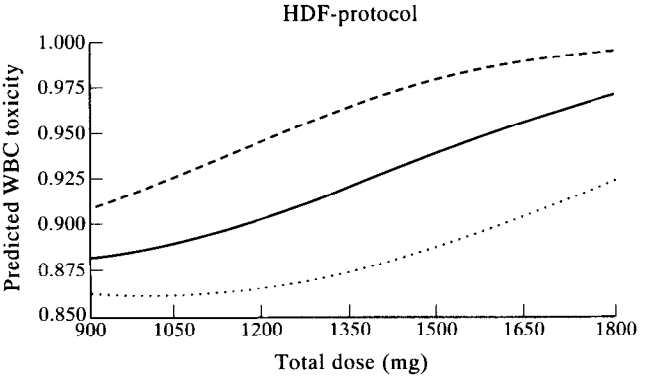

Figure 2. Predictions of WBC toxicities as a function of administered doses for patients receiving the HDF-protocol: ----, Patient 23, CL = 56.43 l/h; ——, Patient 34, CL = 82.93 l/h; ....., Patient 9, CL = 115.4 l/h.

rapidly decomposed into reactive species. This chemical instability is also a drawback when one analyses the unchanged drug in biological fluids. Despite these intrinsic difficulties, the PKs and the PDs of the nitrosourea fotemustine were investigated in depth in the present study. Two different protocols were used: one with conventional dose therapy and the other with high doses. We found that $t_{1/2}$ and V_{dss} were modified according to the type of schedule, probably because of the different blood sampling protocols. However, CL, the most clinically relevant PK parameter, remained unchanged by the protocol used. The mean total CL (91.7 l/h, i.e. 22 ml/min/kg for 70 kg) was much lower than that reported by Levin and associates [23] for BCNU, a structurally related molecule, which averaged 77 ml/min/kg. For a drug like nitrosourea, submitted to extensive biotransformation in the body, it was necessary to check both the stability of the PK parameters during consecutive courses and the effect of the dose increase. The data presented herein indicate that fotemustine CL remained stable during repeated cycles and with doses between 162 and 900 mg. These characteristics are clinically relevant, especially when the hypothesis of proportionality between AUC and dose must be fulfilled in phase I trials so as to apply the pharmacokinetically guided concepts [24, 25].

We thought it of interest to discuss the model of Collins and colleagues [26] in the light of the data available for fotemustine. Previous investigations have shown that, in mice, the LD_{10} is 50 mg/kg (150 mg/m^2) and AUC at the LD_{10} is 9.6 mg/l/h [27], and that mean human AUC at MTD is 3.0 mg/l/h. The same mean AUC was obtained in this study, with a mean CL value of 91.7 l/h. Thus, it clearly appears that, for fotemustine, a discrepancy exists between the AUC at MTD in man and the AUC at LD_{10} in the mouse, since the ratio [AUC(MTD)/AUC(LD_{10})] is 0.3. Moreover, fotemustine doses at LD_{10} in mice and MTD in humans were identical (150 mg/m^2), showing a better species correlation between doses than between AUCs in the case of fotemustine. Similar discrepancies between AUC at MTD in humans and at LD_{10} in mice have been reported by other authors [28], suggesting caution with this theory.

Leucopenia is the limiting toxicity of the nitrosoureas [29]. General studies have provided evidence that systemic exposure to cytotoxic agents is linked to their toxicity, but without a strong relationship between the administered dose

and the toxicity. To our knowledge, no data have been published on the clinical PK–PD relationship of nitrosoureas. Using a quadratic form of the logit regression model to express the PD observations, we have shown that both dose and AUC are useful variables for predicting the intensity of a haematological toxicity, especially in the case of WBC.

The prospective evaluation of the PD model developed here is currently ongoing in new patients entering fotemustine trials. In fact, the analytical method is routinely applicable and sufficiently quick (extraction and detection procedures no longer than 3 h) to obtain PK evaluation and then perform PK–PD modelling in real time. In the same way, the clinical response to the treatment will be recorded and analysed in a large number of patients: this will make it possible to monitor both the toxicity and activity of the compound by using the PK–PD model. If this PK–PD approach proves to be efficient in selecting the optimal individual dosage regimen, one could routinely apply it in the following way: (1) assessment of PK parameters of each individual patient at the first fotemustine administration (CL is thus known), (2) after definition of the maximum haematological toxicity desired for the entire treatment, prediction of the corresponding maximum tolerated AUC using the PD model, and (3) based on the latter and knowing the patient CL, calculation of the maximum dose to be administered during subsequent courses.

Finally, from an ethical and practical point of view, since the PK identification for each patient is mandatory for dosage individualisation, a limited sampling procedure including Bayesian estimation for individual PK identification should be developed [30]. This is also presently being investigated in order to help clinicians in selecting the appropriate fotemustine dosage regimen on the basis of the known PK characteristics of fotemustine.

1. Foster DO, Pardee AB. Transport of amino-acids by confluent and non confluent 3T3 and polyoma virus transformed 3T3 cells growing on glass cover slips. *J Biol Chem* 1969, **244**, 2675–2681.
2. Montgomery JA, Mayo JG, Hansch C. Quantitative structure–activity relationship of anticancer agents. Activity of selected nitrosoureas against a solid tumor: the Lewis lung carcinoma. *J Med Chem* 1974, **17**, 477–480.
3. Tapiero H, Ming-Biao Y, Catalin J, *et al.* Cytotoxicity in DNA damaging effects of a new nitrosourea, fotemustine, diethyl-1-(3-(2-chloroethyl)-3-nitrosoureido) ethylphosphonate-S 10036. *Anticancer Res* 1989, **9**, 1617–1622.
4. Fischel JL, Formento P, Etienne MC, *et al.* In vitro chemosensitivity testing of fotemustine (S 10036), a new antitumor nitrosourea. *Cancer Chemother Pharmacol* 1990, **25**, 337–341.
5. Khayat D, Lokiec F, Bizzari JP, *et al.* Phase I clinical study of the new amino acid-linked nitrosourea, S 10036, administered on a weekly schedule. *Cancer Res* 1987, **47**, 6782–6785.
6. Jacquillat C, Khayat D, Banzet P, *et al.* Final report of the French multicentre phase II study of the nitrosourea fotemustine in 153 evaluable patients with disseminated malignant melanoma including patients with cerebral metastasis. *Cancer* 1990, **66**, 1873–1878.
7. Avril MF, Bonneterre J, Delaunay M, *et al.* Combination chemotherapy of dacarbazine and fotemustine in disseminated malignant melanoma. *Cancer Chemother Pharmacol* 1990, **27**, 81–84.
8. Frenay M, Giroux B, Khoury S, Derlon JM, Namer M. Phase II study of fotemustine in recurrent supratentorial malignant gliomas. *Eur J Cancer* 1991, **27**, 852–856.
9. McDonald JS, Weiss RB, Poster D, Hammershaim B. Subacute and chronic toxicities associated with nitrosoureas therapy. In Prestayko AM, Crooke ST, Baker LH, *et al.*, eds. *Nitrosureas: Current Status and New Developments*. New York, Academic Press, 1981, 145–154.
10. Ings RMJ, Gray AJ, Taylor AR, *et al.* Disposition, pharmacokinetics, and metabolism of ^{14}C-fotemustine in cancer patients. *Eur J Cancer* 1990, **26**, 838–842.
11. Ratain MJ, Schilsky RL, Coney BA, Egorin MJ. Pharmacodynamics in cancer therapy. *J Clin Oncol* 1990, **8**, 1739–1753.
12. Newell DR. Pharmacokinetic determinants of the activity and toxicity of antitumor agents. *Cancer Surveys* 1989, **8**, 557–603.
13. Thyss A, Milano G, Renée N, Vallicioni J, Schneider M, Demard F. Clinical pharmacokinetic study of 5FU in continuous 5-day infusions for head and neck cancer. *Cancer Chemother Pharmacol* 1986, 16, 64–66.
14. Santini J, Milano G, Thyss A, *et al.* 5FU therapeutic monitoring with dose adjustment leads to an improved therapeutic index in head and neck cancer. *Br J Cancer* 1989, **59**, 287–290.
15. Egorin MJ, VanEcho DA, Tipping SJ, *et al.* Pharmacokinetics and dosage reduction of cis-diammine (1,1-cyclobutane dicarboxylate) platinum in patients with impaired renal function. *Cancer Res* 1984, **44**, 5432–5438.
16. Calvert AH, Newell DR, Gumbrell LA, *et al.* Carboplatin dosage: prospective evaluation of a simple formula based on renal function. *J Clin Oncol* 1989, **7**, 1748–1756.
17. Gordon BH, Richards RP, Hiley MP, Gray AJ, Ings RMJ, Campbell DB. A new method for the treatment of nitrosoureas in plasma: an HPLC procedure for the measurement of fotemustine kinetics. *Xenobiotica* 1989, **19**, 329–339.
18. Ilidis A, Brown AC, Huggins ML. APIS: a software for model identification, simulation and dosage regimen calculations in clinical and experimental pharmacokinetics. *Comput Meth Prog Biomed* 1992, **38**, 227–239.
19. Astrom KJ, Eykhoff P. System identification: a survey. *Automatica* 1971, **7**, 123–162.
20. Dixon WJ, Brown MB, Engelman L, *et al.* BMDP Statistical Software, University of California Press, 1985.
21. Evans WE, Relling MV. Clinical pharmacokinetics-pharmacodynamics of anticancer drugs. *Clin Pharmacokinet* 1989, **16**, 327–336.
22. Liliemark J, Peterson C. Pharmacokinetic optimisation of anticancer therapy. *Clin Pharmacokinet* 1991, **21**, 213–231.
23. Levin VA, Hoffman W, Weinkam RJ. Pharmacokinetics of BCNU in man, a preliminary study of 20 patients. *Cancer Treat Rep* 1978, **62**, 1305–1312.
24. Collins JM, Grieshaber CK, Chabner BA. Pharmacologically guided phase I trials based upon preclinical drug development. *J Natl Cancer Inst* 1990, **82**, 1321–1326.
25. EORTC Pharmacokinetics and Metabolism Group. Pharmacokinetically guided dose escalation in phase I clinical trials. *Eur J Cancer Clin Oncol* 1987, **23**, 1083–1087.
26. Collins JM, Zaharko DS, Dedrick RL, Chabner BA. Potential roles of preclinical pharmacology in phase I clinical trials. *Cancer Treat Rep* 1986, **70**, 73–79.
27. Lucas C, Ings RMJ, Gray AJ, *et al.* Interspecies comparison of pharmacokinetic parameters of fotemustine (nitrosourea S 10036): mice, rats, monkeys, dogs and man. *Bull Cancer* 1989, **76**, 863–865.
28. DeJong J, Geijssen GJ, Munniksma CN, Vermorken JB, Van Der Vijgh WJF. Plasma pharmacokinetics and pharmacodynamics of a new prodrug N-1-leucyldoxorubicin and its metabolites in a phase I clinical trial. *J Clin Oncol* 1992, **10**, 1897–1906.
29. Weiss RB, Isbel BF. The nitrosoureas: carmustine (BCNU) and lomustine (CCNU). *Cancer Treat Rev* 1982, **9**, 313–330.
30. Sheiner LB, Beal SL, Rosenberg B, Marathe VV. Forecasting individual pharmacokinetics. *Clin Pharmacol Ther* 1979, **26**, 294–305.

Acknowledgement—This study was supported by grants from I.R.I. Servier Laboratories.